
Hiroshima University Institutional Repository

Microhydration of Dibenzo-18-Crown-6 Complexes with K^+, Rb^+, and Cs^+ Investigated by Cold UV and IR Spectroscopy in the Gas Phase

Yoshiya Inokuchi,[‡,*] Takayuki Ebata,[‡] and Thomas R. Rizzo[†]

Department of Chemistry, Graduate School of Science, Hiroshima University, Higashi-Hiroshima, Hiroshima 739-8526, Japan and Laboratoire de Chimie Physique Moléculaire, École Polytechnique Fédérale de Lausanne, Lausanne CH-1015, Switzerland

E-mail: y-inokuchi@hiroshima-u.ac.jp

Phone: +81 (Japan)-82-424-7101

Abstract

In this paper, we examine the hydration structure of dibenzo-18-crown-6 (DB18C6) complexes with K^+, Rb^+, and Cs^+ ion in the gas phase. We measure well-resolved UV photodissociation (UVPD) spectra of K^+•DB18C6•$(H_2O)_n$, Rb^+•DB18C6•$(H_2O)_n$, and Cs^+•DB18C6•$(H_2O)_n$ (n = 1–8) complexes in a cold, 22-pole ion trap. We also measure IR-UV double-resonance spectra of the Rb^+•DB18C6•$(H_2O)_{1–5}$ and the Cs^+•DB18C6•$(H_2O)_3$ complexes. The structure of the hydrated complexes is determined or tentatively proposed on the basis of the UV and IR spectra with the aid of quantum chemical calculations. Bare complexes (K^+•DB18C6, Rb^+•DB18C6, and Cs^+•DB18C6) have a similar boat-type conformation, but the

distance between the metal ions and the DB18C6 cavity increases with increasing ion size from K^+ to Cs^+. Though the structural difference of the bare complexes is small, it highly affects the manner in which each is hydrated. For the hydrated K^+•DB18C6 complexes, water molecules bind on both sides (top and bottom) of the boat-type K^+•DB18C6 conformer, while hydration occurs only on top of the Rb^+•DB18C6 and Cs^+•DB18C6 complexes. Based on our analysis of the hydration manner of the gas phase complexes, we propose that for Rb^+•DB18C6 and Cs^+•DB18C6 complexes in aqueous solution, water molecules will preferentially bind on top of the boat conformers because of the displaced position of the metal ions relative to DB18C6. In contrast, the K^+•DB18C6 complex can accept H_2O molecules on both sides of the boat conformation. We also propose that the characteristic solvation manner of the K^+•DB18C6 complex will contribute entropically to its high stability and thus to preferential capture of K^+ ion by DB18C6 in solution.

*To whom correspondence should be addressed.

[‡]Hiroshima University

[†]École Polytechnique Fédérale de Lausanne

1. Introduction

Crown ethers are the most common host molecules for ion complexation in supramolecular and organic chemistry.[1] One of their characteristics is the ability to selectively encapsulate certain metal ions. For example, dibenzo-18-crown-6 (DB18C6) selectively captures K^+ among alkali metal ions in aqueous solution.[2-3] One important conclusion derived from our previous studies of ion-crown ether complexes[4-6] is that solvent effects highly control the alkali ion selectivity. In addition, a number of studies suggest the existence of multiple isomers,[7-11] which contributes to the complex stability. In our previous work, we examined the number and the structure of isomers in bare and micro-solvated forms of crown ether complexes by gas-phase spectroscopy and found their relation to the guest selectivity.[4-6, 12-15] We determined the structure of DB18C6 complexes with alkali metal ions, M^+•DB18C6 (M = Li, Na, K, Rb, and Cs) using UV and IR spectroscopy under cold gas-phase conditions.[4] In bare K^+•DB18C6, Rb^+•DB18C6, and Cs^+•DB18C6, the DB18C6 part adopts a similar boat-type open conformation, but the distance between the DB18C6 cavity and the metal ions increases with increasing ion size from K^+ to Cs^+.[4] For microhydrated systems, we reported UV and IR spectra of hydrated K^+•DB18C6 complexes, K^+•DB18C6•$(H_2O)_{1–5}$, in the gas phase.[6] Since the K^+ ion in the K^+•DB18C6 complex is encapsulated deeply with the crown cavity, H_2O molecules can bind directly to the K^+ ion on both (top and bottom) sides of the boat-type K^+•DB18C6 conformer. This hydration manner is due to the optimum matching in size between the DB18C6 cavity and the K^+ ion.

In the present work, we extend our investigation of hydrated complexes to larger alkali-metal ions; that is Rb^+•DB18C6 and Cs^+•DB18C6 complexes. As mentioned above, bare K^+•DB18C6, Rb^+•DB18C6, and Cs^+•DB18C6 complexes have a

similar boat-type structure, but the position of the metal ions with respect to the DB18C6 part is slightly different from each other.[4] We examine how the difference in the metal position, or difference in the matching in size between the DB18C6 cavity and the metal ions, affects the manner of hydration.

2. Experimental and computational methods

The details of our experimental approach have been given elsewhere.[4, 6, 16] Briefly, the K^+•DB18C6•$(H_2O)_n$, Rb^+•DB18C6•$(H_2O)_n$ and Cs^+•DB18C6•$(H_2O)_n$ (n = 1–8) complexes are produced continuously at atmospheric pressure *via* nanoelectrospray of a solution containing KCl, RbCl, or CsCl and DB18C6 (~10 μM each) dissolved in methanol/water (~9:1 volume ratio). The parent ions of interest are selected in a quadrupole mass filter and injected into a 22-pole RF ion trap, which is cooled by a closed-cycle He refrigerator to 6 K. The trapped ions are cooled internally and translationally to ~10 K through collisions with cold He buffer gas,[4, 16-18] which is pulsed into the trap. The trapped ions are then irradiated with a UV laser pulse, which causes some fraction of them to dissociate. The resulting charged photofragments, as well as the remaining parent ions, are released from the trap, mass-analyzed by a second quadrupole, and detected with a channeltron electron multiplier. Ultraviolet photodissociation (UVPD) spectra of parent ions are obtained by plotting the yield of the photofragment ion as a function of the UV laser wavenumber. The UVPD spectra of the M^+•DB18C6•$(H_2O)_n$ (M = K, Rb, and Cs) complexes are measured by monitoring the yield of the bare M^+•DB18C6 photofragment ion, since it is a dominant photodissociation product and is hardly affected by the metastable decay of the parent ions between the first quadrupole and the 22-pole ion trap. For IR-UV double-resonance spectroscopy, the output pulse of an IR OPO precedes the UV pulse

by ~100 ns and counter-propagates collinearly with it through the 22-pole trap. Absorption of the IR light by the ions warms them up, modifying their absorption.[19] We obtain IR-UV depletion and gain spectra by tuning the wavenumber of the UV laser either to the vibronic transition of a specific conformer or to a non-resonant position, respectively. The IR-UV depletion spectra provide conformer-selective IR spectra, whereas the IR-UV gain spectra represent the overall IR absorption due to all the isomers present in the experiment.

For geometry optimization of the M^+•DB18C6•$(H_2O)_n$ (M = K, Rb, and Cs) complexes, we first use a classical force field to find conformational minima. The initial conformational search is performed by using the mixed torsional search with low-mode sampling and the AMBER* force field as implemented in MacroModel V. 9.1.[20] Minimum-energy conformers found with the force field calculations are then optimized at the M05-2X/6-31+G(d) level and successively at the M05-2X/6-311++G(d,p) level using the GAUSSIAN09 program package.[21] Vibrational analysis is carried out for the optimized structures at the M05-2X/6-311++G(d,p) level. Calculated frequencies at the M05-2X/6-311++G(d,p) level are scaled with a factor of 0.9425 for comparison with the IR-UV spectra. This factor was determined so as to simulate the IR spectrum of the K^+•DB18C6•$(H_2O)_1$ complex.[6] All stable conformers are named systematically using "Rb1a" notation, where the first letters indicate the metal ion of a complex, the subsequent number represents the number of the attached H_2O molecules, and the final lower case letter stands for the stability order of conformers determined at the M05-2X/6-311++G(d,p) level with zero-point energy correction. For Rb and Cs, we use the Stuttgart RLC as effective core potentials (ECPs); functions of the ECPs are obtained from a database of basis sets.[22]

3. Results

3.1. UVPD spectra

Figure S1 of the Supporting Information displays the UVPD spectra of the K^+•DB18C6•$(H_2O)_n$ (n = 0–8) complexes in the 35800–36600 cm^{-1} region. All the spectra in Figure S1 consist of sharp bands with different vibronic patterns. The UV spectrum of bare K^+•DB18C6 (Figure S1a) has its band origin at 36415 cm^{-1},[4] which is 700 cm^{-1} higher than that of jet-cooled neutral DB18C6 monomer.[23] The spectra of the hydrated complexes are also higher in energy than the DB18C6 monomer,[23-24] although to a lesser degree. The relative band positions of the UV absorption of the K^+•DB18C6•$(H_2O)_n$ complexes reflect the strength of the intermolecular interaction between DB18C6 and the other components in the complexes. The UV spectra of the n = 1–4 complexes increasingly shift to the red with increasing cluster size, which suggests a progressive decrease in the intermolecular interaction with DB18C6. For the n = 5 complex, the vibronic bands shift to higher frequency again, followed by a gradual shift to lower frequency for complexes with n = 6 to 8. Another noticeable feature of this series of UVPD spectra is that the n = 4 complex shows highly congested features compared to those of the other complexes.

Figure S2 of the Supporting Information shows the UVPD spectra of the Rb^+•DB18C6•$(H_2O)_n$ (n = 0–8) complexes, which exhibit a similar trend as the corresponding potassiated species. The 0-0 band in the spectrum of Rb^+•DB18C6 (Figure S2a) appears at 36319 cm^{-1},[4] with those of the hydrated complexes progressively shifting to lower energy for n = 1 to 4 before shifting to higher frequency again at n = 5. The UVPD spectrum of the n = 4 complex (Figure S2e) shows congested features, similar to that of the K^+•DB18C6•$(H_2O)_4$ complex (Figure S1e).

Unlike the case of the doubly hydrated potassiated species (Figure S1c), the Rb^+•DB18C6•$(H_2O)_2$ complex shows congested spectral features with no strong origin band (Figure S2c).

The UVPD spectra of the Cs^+•DB18C6•$(H_2O)_n$ (n = 0–8) complexes are shown in Figure S3 of the Supporting Information. The origin band of Cs^+•DB18C6 appears at 36234 cm^{-1} (Figure S3a).[4] Similar to K^+ and Rb^+, the UV bands of the Cs^+ complexes shift to lower frequency with increasing hydration. However, one difference for the Cs^+ spectra (Figure S3) from the K^+ and Rb^+ spectra (Figures S1 and S2) is that the UV bands continuously shift to lower frequency from n = 1 to 5 before exhibiting a blue shift at n = 6. Moreover, in the case of the Cs^+ complexes, it is the n = 5 species (Figure S3f) that exhibits particularly congested vibronic features. In the spectra of the n = 2 and 4 complexes (Figures S3c and S3e), a number of sharp bands appear much more closely than the case of Rb^+. These spectral features will represent the complex structure, which will be described in more detail in following sections.

3.2. Computed structures

Figure 1 shows optimized computed structures of the M^+•DB18C6•$(H_2O)_n$ (M = K, Rb, Cs; n = 1–5) complexes obtained at the M05-2X/6-311++G(d,p) level. We have previously determined the structure of bare complexes (K-a, Rb-a, and Cs-b),[4] and have confirmed that the conformers of the hydrated K^+•DB18C6 complexes shown in Figure 1 exist in the experiment under cold gas-phase conditions.[6] For the hydrated Rb^+•DB18C6 and Cs^+•DB18C6 complexes, the most stable conformers (or the second most stable conformer for Cs^+•DB18C6•$(H_2O)_1$) are displayed in Figure 1. The most and the second most stable structures of the M^+•DB18C6•$(H_2O)_n$ complexes are shown with the total energy in Figures S4–8 of the Supporting Information. All the

complexes in Figure 1 have a boat-type form in the M^+•DB18C6 part. In all the isomers of the Rb^+•DB18C6•$(H_2O)_n$ and Cs^+•DB18C6•$(H_2O)_n$ complexes, the H_2O molecules are located only on top of a boat-type M^+•DB18C6 conformer, even for the complexes smaller than n = 4; the K^+•DB18C6•$(H_2O)_{2,3}$ complexes have the H_2O molecules on both sides of the boat K^+•DB18C6 conformer (Figure 1). This is in strong contrast to the K^+•DB18C6•$(H_2O)_n$ (n = 1–3) complexes, where the H_2O molecules are located either on top or bottom, or on both sides.[6] As will be demonstrated below, we propose the structure of the hydrated complexes on the basis of UVPD and IR-UV spectra, not of the stability order of isomers in quantum chemical calculations. The calculated total energy of the conformers cannot be used as a definitive evidence for the structural assignment of the complexes, because it highly depends on the calculation level.

3.3. IR spectra

We have reported conformer-selective, IR-UV double-resonance spectra of the K^+•DB18C6•$(H_2O)_n$ (n = 1–5) complexes in our previous study.[6] The smaller abundance of the hydrated Rb^+•DB18C6 and Cs^+•DB18C6 complexes prevented us from measuring exhaustive IR-UV spectra, but we have succeeded in obtaining spectra for some of them. Figure 2 shows the IR-UV (red curves) and theoretical IR (black curves and bars) spectra of the Rb^+•DB18C6•$(H_2O)_n$ (n = 1–3) complexes in the OH stretching region. Black bars present calculated results of the oscillator strength and vibrational frequency, and black curves are produced by distributing a Lorentzian function with intensity proportional to the oscillator strength and a fwhm of 5 cm^{-1} to each vibration. The UV probe positions at which the IR-UV spectra are measured are shown with arrows in Figure S2 of the Supporting Information. The top curves in

Figures 2a–c are the IR-UV gain spectra measured at non-resonant UV positions, which should reflect the IR spectra of all conformers present in the experiment. In the case of the n = 1 complex (Figure 2a), the signal to noise ratio of the gain spectrum is not so high, but it gives two IR bands at 3609 and 3712 cm^{-1}, which are highlighted by arrows. The calculated IR spectrum of isomer Rb1a (Figure 1) well reproduces the obtained gain spectrum. The second most stable isomer (Rb1b, Figure S5 of the Supporting Information) has a characteristic IR band at 3565 cm^{-1}. This band corresponds to the stretching vibration of the OH group hydrogen-bonded to an ether oxygen. In the IR-UV gain spectrum, no strong band is observed around 3560 cm^{-1}, suggesting that isomer Rb1b is not present in the experiment.

For the n = 2 complex, the IR-UV gain spectrum (top spectrum in Figure 2b) shows bands at 3608 and 3716 cm^{-1}, but no band is found in the 3400–3600 cm^{-1} region. This IR-UV gain spectrum is quite similar to the theoretical one of isomer Rb2a (Figure 1). The second most stable isomer (Rb2b, Figure S5 of the Supporting Information) is predicted to have a strong band at 3449 cm^{-1} due to the stretching vibration of the hydrogen-bonded OH group. However, the IR-UV gain spectrum shows no such band, indicating the absence of isomer Rb2b in the experiment.

Infrared spectra of the Rb^+•DB18C6•$(H_2O)_3$ complex are shown in Figure 2c.[6] The IR-UV gain spectrum (top spectrum in Figure 2c) shows peaks at 3520, 3528, 3558, 3696, and 3709 cm^{-1}, accompanied by a weak shoulder at 3713 cm^{-1}. We measure IR-UV dip spectra at two resonant UV positions (36032 and 36182 cm^{-1}). The IR-UV depletion spectrum measured at 36032 cm^{-1} clearly shows five dips at the same positions with those of the gain spectrum. This indicates that the IR-UV bands of the n = 3 complex are due to a single isomer. The depth is not high, but the IR-UV

spectrum at 36182 cm^{-1} is similar to that measured at 36032 cm^{-1}, confirming the presence of a single conformer. The spectral pattern of the theoretical IR spectrum of isomer Rb3a (Figure 1) well reproduces the observed IR-UV spectra, exhibiting three bands around 3500 cm^{-1} and two bands around 3700 cm^{-1}. In contrast, the spectral features of the second most stable isomer (Rb3b, Figure S5 of the Supporting Information) are sufficiently different from those of the measured spectra. From these results, the IR-UV spectra of the n = 1–3 complexes can be described by theoretical IR spectra of the most stable isomers (Rb1a, Rb2a, and Rb3a).

Figure 3 displays the IR-UV (red curves) and theoretical IR (black curves and bars) spectra of the Rb^+•DB18C6•$(H_2O)_{4, 5}$ complexes. In the IR-UV gain spectrum of the n = 4 complex (top spectrum of Figure 3a), peaks are seen at ~3445, ~3460, 3660, and 3708 cm^{-1}. The most stable isomer of the n = 4 complex (Rb4a, Figure 1) reproduces the IR spectrum with peaks at 3450, 3453, 3663, and 3723 cm^{-1}. The IR-UV gain spectrum of the n = 5 complex (Figure 3b) has broad absorption in the 3300–3500 cm^{-1} region and a weak one at ~3575 cm^{-1}. These spectral patterns are reasonably well reproduced by the calculated IR spectrum of isomer Rb5a (Figure 1).

Figure 4 presents the IR-UV (red curves) and theoretical IR (black curves and bars) spectra of the Cs^+•DB18C6•$(H_2O)_3$ complex, reproduced from our previous paper.[6] The IR-UV gain and dip spectra (top two spectra of Figure 4) are similar to each other; IR bands are found at 3511, 3524, 3553, 3694, and 3705 cm^{-1}. Therefore, the IR-UV gain spectrum of the Cs^+•DB18C6•$(H_2O)_3$ complex is attributed to a single isomer. The spectral patterns of the IR-UV spectra of the Cs^+•DB18C6•$(H_2O)_3$ complex resemble those of the Rb^+•DB18C6•$(H_2O)_3$ complex (Figure 2c). In addition, the most stable calculated isomer (Cs3a, Figure 1) shows an IR spectrum similar to that

we measure. In the following section, we discuss the probable structure of the M^+•DB18C6•$(H_2O)_n$ complexes on the basis of the UVPD, IR-UV, and theoretical results described above.

4. Discussion

4.1. M^+•DB18C6•$(H_2O)_1$ complexes

In our previous work, we determined the hydration structure of the K^+•DB18C6•$(H_2O)_{1–5}$ complexes by IR spectroscopy in the OH stretching region.[6] Here we determine structure of the hydrated Rb^+•DB18C6 and Cs^+•DB18C6 complexes using a combination of UVPD and IR spectra. Figure 5 displays the UVPD spectra of the M^+•DB18C6•$(H_2O)_1$ (M = K, Rb, and Cs) complexes for comparison. For the K^+•DB18C6•$(H_2O)_1$ complex, all the bands are attributed to a single isomer (K1a, Figure 1).[6] In this isomer, the oxygen atom of the H_2O molecule is directly attached to the K^+ ion, and one of the OH groups forms the O–H•••π hydrogen bond with one of the benzene rings. As a result, the two benzene rings are not equivalent. Time-dependent density functional theory (TD-DFT) calculations of the K^+•DB18C6•$(H_2O)_1$ complex predicts that the S_1–S_0 and S_2–S_0 transition energies of isomer K1a differ by more than 100 cm^{-1}, and the S_1–S_0 transition is localized almost entirely on the benzene ring involved in the O–H•••π hydrogen bond. In addition, the vibronic structures starting from 36274 and 36334 cm^{-1} show different features from each other (an expanded view of the UVPD spectrum is shown in Figure S11 of the Supporting Information). Based on these theoretical and experimental results, the two strong bands observed at 36274 and 36334 cm^{-1} (Figure 5a) can be reasonably assigned to the 0-0 band of the S_1–S_0 and S_2–S_0 transitions.

The structure of the Rb^+•DB18C6•$(H_2O)_1$ complex should be similar to that of the K^+•DB18C6•$(H_2O)_1$ complex, because the IR-UV spectrum of the former (Figure 2a) in the region of the OH stretching bands strongly resembles that of the latter (Figure 2a of ref. 6). Moreover, isomer Rb1a of the Rb^+ complex (Figure 1) has a structure similar to that of the K^+ complex determined in our pervious paper (K1a, Figure 1).[6] We thus assign the structure of isomer Rb1a in Figure 1 to the Rb^+•DB18C6•$(H_2O)_1$ complex. We also suppose that the strong sharp band observed at 36260 cm^{-1} in the UVPD spectrum of Rb^+•DB18C6•$(H_2O)_1$ (Figure 5b) is the 0-0 band of the S_2–S_0 transition, which would make the weak band 36165 cm^{-1} the 0-0 band of the S_1–S_0 transition. As mentioned above, the S_1–S_0 transition of the K^+•DB18C6•$(H_2O)_1$ complex is mainly localized in the benzene ring having the O–H•••π hydrogen bond, and a similar localization can be seen also in the calculation of Rb^+•DB18C6•$(H_2O)_1$.

While an IR spectrum is not available for the Cs^+•DB18C6•$(H_2O)_1$ complex, it is possible to infer the structure on the basis of the UVPD spectrum. As shown in Figure 5c, the UVPD spectrum of the Cs^+•DB18C6•$(H_2O)_1$ complex is quite similar to that of the corresponding Rb^+ complex. A strong, sharp band is observed at 36181 cm^{-1}, which can be attributed to the 0-0 band of the S_2–S_0 transition, and we assign the weak band at 36075 cm^{-1} to the 0-0 band of the S_1–S_0 transition. The amount of the red-shift from Rb^+•DB18C6•$(H_2O)^+$ to Cs^+•DB18C6•(H_2O) is ~85 cm^{-1}, which is comparable to that between unsolvated Rb^+•DB18C6 and Cs^+•DB18C6 (85 cm^{-1}).[4] The similarity of this spectrum to that of the Rb^+ complex indicates a similar structure. The two most stable isomers of the Cs^+•DB18C6•$(H_2O)_1$ complex are shown in Figure S7 of the Supporting Information. Among them, isomer Cs1b (Figure 1) has a structure similar to that of Rb^+•DB18C6•$(H_2O)_1$ (Rb1a, Figure 1). Hence, we assign the structure of Cs^+•DB18C6•$(H_2O)_1$ to isomer Cs1b. Isomer Cs1b (Figure 1) is the

second most stable structure of the Cs^+•DB18C6•$(H_2O)_1$ complex at the M05-2X/6-311++G(d,p) level. The DB18C6 has a boat-type open conformation, while in the most stable structure, Cs1a (Figure S7), a part of the DB18C6 ring is bent. Similar conformers (Cs-a and Cs-b) were also found in quantum chemical calculations of bare Cs^+•DB18C6,[4] which we determined to adopt the boat-type C_{2v} conformer (Cs-b) on the basis of the UV spectrum; Cs-b well reproduces the position of the 0-0 band in the UVPD spectrum, and Cs-a has a transition energy more than 500 cm^{-1} higher than that of Cs-b.[4] Since the UV absorption of the Cs^+•DB18C6•$(H_2O)_n$ complexes shifts to lower frequency from n = 0 to 1 (Figures S3a and b), the Cs^+•DB18C6 part in the Cs^+•DB18C6•$(H_2O)_1$ complexes should have a boat-type conformation similar to the structure of bare Cs^+•DB18C6 (Cs-b). Thus, isomer Cs1b is the most likely form for the Cs^+•DB18C6•$(H_2O)_1$ complex. Here it should be emphasized again that the structural assignment for the n = 1 complexes described above is performed on the basis of the experimental UV and IR spectra, not of the calculated total energy of the isomers; isomers K1a and Rb1a (Figure 1), which are determined to be present in the experiment, are the most stable for the K^+•DB18C6•$(H_2O)_1$ and Rb^+•DB18C6•$(H_2O)_1$ complexes at the M05-2X/6-311++G(d,p) level, though the stability order of the isomers may be changed at different calculation levels.

4.2. M^+•DB18C6•$(H_2O)_2$ complexes

The UVPD spectra of the M^+•DB18C6•$(H_2O)_2$ (M = K, Rb, and Cs) complexes are compared in Figure 6. The spectral patterns are quite different between the K^+ and Rb^+ complexes. The UVPD spectrum of the K^+•DB18C6•$(H_2O)_2$ complex (Figure 6a), appears relatively simple, with two sharp origin bands at 36267 and 36326

cm^{-1}. In contrast, the UVPD spectrum of the Rb^+•DB18C6•$(H_2O)_2$ complex (Figure 6b) exhibits a congested progression with many sharp bands. The qualitative difference in the UVPD spectra of the K^+ and Rb^+ complexes suggest that they have substantially different structures. On the basis of previously measured IR-UV spectra of the K^+ complex,[6] the UVPD bands at 36267 and 36326 cm^{-1} have been assigned to two different isomers (K2f and K2d, respectively, Figure 1). These spectra show a strong IR band at ~3453 cm^{-1}, which is assigned to the stretching vibration of the OH group hydrogen-bonded to the other H_2O molecule.[6] These two H_2O molecules are bound on top or on the bottom of the boat-type K^+•DB18C6 conformer. In contrast, the IR-UV gain spectrum of the Rb^+•DB18C6•$(H_2O)_2$ complex, shown in Figure 2b, does not exhibit a band around 3450 cm^{-1}; the IR band positions of the Rb^+•DB18C6•$(H_2O)_2$ complex (3608 and 3716 cm^{-1}) are almost the same as that of Rb^+•DB18C6•$(H_2O)_1$ (3609 and 3712 cm^{-1}, Figure 2a). Hence, the two H_2O molecules in the Rb^+•DB18C6•$(H_2O)_2$ complex appear to be bound independently to the Rb^+•DB18C6 in a manner similar to that in the Rb^+•DB18C6•$(H_2O)_1$ complex. As seen in Figure 1, isomer Rb2a of the Rb^+•DB18C6•$(H_2O)_2$ complex has a hydration structure similar to that of Rb^+•DB18C6•$(H_2O)_1$ (Rb1a, Figure 1). The calculated IR spectrum of isomer Rb2a well reproduces the band position of the measured spectrum (Figure 2b). We conclude that the Rb^+•DB18C6•$(H_2O)_2$ complex has the structure of isomer Rb2a in Figure 1. The two benzene rings in this isomer are equivalent, leading to a complex with C_2 symmetry. This may enhance the exciton coupling between the two benzene rings leading to congested spectral features, as seen for the bare M^+•DB18C6 (M = K, Rb, and Cs) complexes and for K^+•DB18C6•$(H_2O)_4$.[4, 6]

We consider now the structure of the Cs^+•DB18C6•$(H_2O)_2$ complex on the basis of the UVPD spectrum and the theoretical calculations. The UVPD spectrum of

Cs^+•DB18C6•$(H_2O)_2$ (Figure 6c) more closely resembles that of Rb^+•DB18C6•$(H_2O)_2$ complex rather than that of K^+•DB18C6•$(H_2O)_2$; with many sharp, closely spaced bands. Isomer Cs2a of Cs^+•DB18C6•$(H_2O)_2$ (Figure 1) has a structure similar to that of the Rb^+•DB18C6•$(H_2O)_2$ complex (Rb2a, Figure 1). Hence, we tentatively ascribe the structure of Cs^+•DB18C6•$(H_2O)_2$ to isomer Cs2a; definitive assignment with IR-UV spectroscopy, which includes further improvement of detection efficiency of the photodissociation spectrometer, is our future work.

4.3. M^+•DB18C6•$(H_2O)_3$ complexes

Figure 7 displays UVPD spectra of the M^+•DB18C6•$(H_2O)_3$ (M = K, Rb, and Cs) complexes. In contrast to the spectra of the n = 2 complexes (Figure 6), the spectral features of the n = 3 species are similar among the different cations (i.e., K^+, Rb^+, and Cs^+). The spectra are not as congested as that of Rb^+•DB18C6•$(H_2O)_2$ and Cs^+•DB18C6•$(H_2O)_2$, and the vibronic structure starts with a strong band assignable to the 0-0 transition. The similarity of the UVPD spectra in Figure 7 suggests a similarity of the structures for the K^+, Rb^+ and Cs^+ complexes. In the case of K^+•DB18C6•$(H_2O)_3$, two strong UV bands are found at 36108 and 36223 cm^{-1} (Figure 7a). On the basis of the IR-UV experiments, these UV bands are assigned to the same isomer (K3a, Figure 1),[6] in which all the three H_2O molecules are located on top of the boat-type K^+•DB18C6 conformer. Two of the H_2O molecules are directly bound to the K^+ ion, and the third accepts hydrogen bonds from the other two, while donating an O–H•••π hydrogen bond to one of the benzene rings. The two benzene rings in K3a are not equivalent; TD-DFT calculations show that the S_1–S_0 and S_2–S_0 electronic transitions of K3a are localized in either of the benzene rings and appear at different UV frequencies. In addition, the vibronic structures starting from 36108 and 36223 cm^{-1}

show different features from each other. Hence, the bands at 36108 and 36223 cm^{-1} can be assigned to the 0-0 band of the S_1–S_0 and S_2–S_0 transitions of isomer K3a, respectively. Isomers Rb3a and Cs3a of the Rb^+ and Cs^+ complexes (Figure 1) resemble isomer K3a, and their IR-UV spectra (red curves in Figures 2c and 4) are similar to those of the K^+ complex (Figure 5b of ref. 6). Moreover, the calculated IR spectra of Rb3a and Cs3a well reproduce the measured IR-UV spectra of the Rb^+•DB18C6•$(H_2O)_3$ and Cs^+•DB18C6•$(H_2O)_3$ complexes (Figure 2c and Figure 4, respectively). Hence, we attribute the structure of the Rb^+•DB18C6•$(H_2O)_3$ and Cs^+•DB18C6•$(H_2O)_3$ complexes to isomers Rb3a and Cs3a, respectively (Figure 1). The strong bands observed at 36033 and 36182 cm^{-1} for Rb^+ (Figure 7b) and at 35916 and 36122 cm^{-1} for Cs^+ (Figure 7c) are assigned to the origin band of the S_1–S_0 and S_2–S_0 transitions. In the case of the K^+•DB18C6•$(H_2O)_3$ complex, there appears to be another isomer,[6] which exhibits a sharp UVPD band at 36390 cm^{-1} (highlighted by an arrow in Figure 7a). The structure of this isomer was determined to be isomer K3g (Figure 1) on the basis of its IR spectrum.[6] In this isomer, two H_2O molecules are bound on top of the boat-type K^+•DB18C6, and the other is bound on the bottom. This isomer shows a strong IR-UV band at 3463 cm^{-1}, which does not seem to have an equivalent in the IR-UV spectrum of the Rb^+•DB18C6•$(H_2O)_3$ complex (top panel of Figure 2c). We conclude that the Rb^+ complex does not have an isomer analogous to K3g of the K^+ complex.

4.4. M^+•DB18C6•$(H_2O)_n$ (n = 4–8) complexes

Figure 8 shows the UVPD spectra of the M^+•DB18C6•$(H_2O)_4$ (M = K, Rb, and Cs) complexes. The spectra of the K^+ and Rb^+ complexes (Figure 8a and b) both exhibit congested features with a number of sharp bands, suggesting a similarity of

structure. In the previous study, the structure of the K^+•DB18C6•$(H_2O)_4$ complex was determined to be an isomer in which a ring of four H_2O molecules is bound on top of the boat-type K^+•DB18C6 (K4a in Figure 1).[6] Isomer Rb4a of the Rb^+ complex (Figure 1) has a structure similar to that of K4a, and its calculated IR spectrum well reproduces the IR-UV spectrum of the Rb^+ complex (Figure 3a). Hence, the Rb^+•DB15C5•$(H_2O)_4$ complex is likely to have the structure of isomer Rb4a.

Figure 9 displays the UVPD spectra of the M^+•DB18C6•$(H_2O)_5$ (M = K, Rb, and Cs) complexes. The spectra of the K^+ and Rb^+ complexes each have a strong band assignable to the 0-0 transition, at 36154 and 36096 cm^{-1}, respectively, and the similarity of the UVPD spectra suggests a similarity of their structures. In our previous study, the structure of the K^+•DB18C6•$(H_2O)_5$ complex was determined to be K5a (Figure 1).[6] Given that isomer Rb5a of the Rb^+ complex (Figure 1) is similar to K5a, and the calculated IR spectrum of this isomer reproduces the IR-UV spectrum of the Rb^+•DB18C6•$(H_2O)_5$ complex (Figure 3b), we attribute its structure to isomer Rb5a.

In contrast to the case of the Rb^+ complexes, the UV spectral features of Cs^+•DB18C6•$(H_2O)_{4,5}$ are substantially different from those of the K^+ complexes (Figures 8 and 9). The UVPD spectrum of Cs^+•DB18C6•$(H_2O)_4$ (Figure 8c) does not show extensive vibrational progressions as do the corresponding K^+ and Rb^+ complexes. In the case of Cs^+•DB18C6•$(H_2O)_5$, the UVPD spectrum (Figure 9c) seems to consist of a number of broad bands, whereas the corresponding K^+ and Rb^+ species show much simpler features with a strong 0-0 band. Since we do not have IR spectra of the Cs^+•DB18C6•$(H_2O)_{4,5}$ complexes, it is difficult to determine their structure definitely. However, as seen in Figure 1, the optimized structures of the Cs^+•DB18C6•$(H_2O)_{4,5}$ complexes (Figures 1, S7, and S8) have a structure different from those of the K^+ (K4a

and K5a) and Rb^+ (Rb4a and Rb5a) species. In isomer Cs4a, the four-membered ring of the H_2O molecules is hydrogen-bonded to one of the oxygen atoms in the DB18C6 part, while in isomers K4a and Rb4a the four-membered ring is bound right on top of the metal ion, apart from the crown cavity. The difference in the structure between Cs5a and K5a or Rb5a is not so obvious; in all of these isomers a five-membered H_2O ring is bound to the metal ions. However, since the radius of the Cs^+ ion is larger than that of K^+ and Rb^+, the position of the H_2O ring relative to the M^+•DB18C6 component in isomer Cs5a is substantially different from that in K5a and Rb5a. These calculations of the Cs^+ complexes are consistent with the UVPD spectra in Figures 8 and 9. We thus tentatively suggest that the Cs^+•DB18C6•$(H_2O)_{4,5}$ complexes can have a structure like Cs4a and Cs5a, respectively. It should be noted that this is a tentative assignment for the n = 4 and 5 complexes of Cs^+ on the basis of the geometry optimization calculated at the M05-2X/6-311++G(d,p) level. Definitive determination of the structure by IR-UV spectroscopy and higher-level calculations is our future work.

The UVPD spectra of the M^+•DB18C6•$(H_2O)_{6–8}$ (M = K, Rb, and Cs) complexes are shown in Figures S1–3 of the Supporting Information. Since the attachment of the metal ions to bare DB18C6 shifts the UV absorption to the blue, the UV band position or the amount of the blue shift can represent a strength scale of the intermolecular interaction that the DB18C6 part has in the M^+•DB18C6•$(H_2O)_n$ complexes.[4] One of the overall trends in the UV spectra of the complexes investigated in this work is that the band position gradually shifts to the red with increasing numbers of water molecules, which indicates that the interaction that the DB18C6 part has becomes weaker and weaker with increasing the hydration number, but then at some point shifts back to the blue before continuing to redshift at still higher hydration. This jump back to higher energy occurs between n = 4 and 5 for the K^+ and Rb^+ complexes

and between n = 5 and 6 for the Cs^+ complexes. This trend in the UVPD spectra is related to the hydration manner in hydrated alkali metal ions, $M^+•(H_2O)_n$. Miller and Lisy reported the structure of hydrated alkali metal ions determined by IR spectroscopy in the gas phase.[25-26] They found that the $K^+•(H_2O)_4$ complex has a four-membered H_2O ring, indicating that this ring size is suitable for effective hydration to K^+ ion. In the case of the $K^+•(H_2O)_5$ complex, four water molecules form a ring through four O–H•••O hydrogen bonds, and this ring is bound to the K^+ ion. The other H_2O molecule is bound to the K^+ ion on the opposite side of the H_2O ring.[25-26] This result suggests that in binding to the K^+ ion, a ring with four H_2O molecules is preferred over a ring with five H_2O molecules. For the K^+•DB18C6•$(H_2O)_n$ (n = 4 and 5) complexes, all the H_2O molecules are bound on top of the K^+•DB18C6 part, forming a ring (Figure 1); the K^+ ion is located between the H_2O ring and the DB18C6 component. The binding ability of H_2O rings to the K^+ ion seems to affect in turn the interaction between the DB18C6 part and K^+ in these complexes. In the K^+•DB18C6•$(H_2O)_4$ complex (K4a in Figure 1), the four-membered H_2O ring attracts strongly the K^+ ion, which can weaken the interaction between the K^+ ion and the DB18C6 part and provide the least blue-shifted UV absorption of DB18C6 among the n = 0–8 complexes (Figure S1). As expected from the hydration manner in $K^+•(H_2O)_5$, the binding strength of the five-membered H_2O ring to the K^+ ion is smaller than that of the four-membered species. Weaker interaction of the K^+ ion with the five-membered H_2O ring results in stronger interaction with the DB18C6 part, showing the blue shift of the DB18C6 absorption at n = 5 (Figure S1). For the Cs^+ ion, the most stable isomer of the $Cs^+•(H_2O)_5$ complex has a ring consisting of five H_2O molecules[26]. This indicates that a five-membered ring is preferred over a four-membered ring for complex formation with Cs^+ ion. The UVPD spectra of the Cs^+•DB18C6•$(H_2O)_n$ complexes show the red shift from n = 0 up

to 5, but the UV absorption shifts to the blue again for n = 6. The intermolecular interaction of the Cs^+ ion with a six-membered ring is likely to be weaker than that with a five-membered ring. As a result, the interaction of the Cs^+ ion with the DB18C6 component becomes stronger for the n = 6 ion.

4.5. Hydration profiles characteristic of M^+•DB18C6 (M = K, Rb, and Cs) complexes

Figure 1 displays the structure of the M^+•DB18C6•$(H_2O)_{0–5}$ (M = K, Rb, and Cs) complexes determined or tentatively proposed in the previous and present studies.[4, 6] The bare complexes, M^+•DB18C6 (M = K, Rb, and Cs) all adopt the boat conformation (K-a, Rb-a, and Cs-b) in which the cavity of the DB18C6 is most open, and the metal ions are located almost at the center of the cavity. The difference in the structure among the bare complexes is the distance between the crown cavity and the metal ions. This small difference leads to a remarkable difference in the structure of the hydrated species. For the n = 1 complexes, the structure is similar for K^+, Rb^+, and Cs^+ (K1a, Rb1a, and Cs1b). For n = 2, Rb^+ and Cs^+ complexes have a similar hydration structure (Rb2a and Cs2a); the two H_2O molecules are bound to Rb^+ or Cs^+ independently and form an O–H•••π hydrogen bond. In contrast, the K^+•DB18C6•$(H_2O)_2$ complex has two types of hydration structure, both different from that of the Rb^+ and Cs^+ complexes; the two H_2O molecules are bound to each other through an O–H•••O hydrogen bond, and are located either on top (K2d) or at the bottom (K2f) of the boat type K^+•DB18C6 conformer. The K^+•DB18C6•$(H_2O)_3$, Rb^+•DB18C6•$(H_2O)_3$, and Cs^+•DB18C6•$(H_2O)_3$ complexes all have a similar hydration structure. One of the two isomers of the K^+ complex (K3a) and the isomers of the Rb^+ and Cs^+ complexes (Rb3a and Cs3a) have all the three H_2O molecules on top of the

M^+•DB18C6 part with a similar hydration structure. The K^+•DB18C6•$(H_2O)_3$ complex has an additional isomer (K3g) with two H_2O molecules on top and one at the bottom of the boat K^+•DB18C6 conformer. For the n = 4 and 5 complexes, the K^+ and Rb^+ complexes have a similar structure to each other (K4a and Rb4a, and K5a and Rb5a), while the Cs^+ complexes have different hydration pattern (Cs4a and Cs5a). We display top views of the n = 4 and 5 complexes in Figures S9 and S10 of the Supporting Information for a closer look at the difference in the structure. In the case of the n = 5 complexes, one of the five H_2O molecules is bound to an oxygen atom of the DB18C6 component; we label this H_2O with "1" and other ones successively with "2–5" in Figure S10. For the K^+ and Rb^+ complexes, the third and fifth H_2O molecules are close to the benzene rings, forming the O–H•••π hydrogen bond. In contrast, the distance between the H_2O ring and the benzene rings is substantially longer for the Cs^+ complex than that for the K^+ and Rb^+ complexes because the Cs^+ ion is displaced largely from the DB18C6 part.

Because the K^+ ion is encapsulated deeply in the DB18C6 cavity, H_2O molecules can be bound to the K^+ ion on both sides of the K^+•DB18C6 complex, which results in multiple isomers in both experiment and theory. For the Rb^+ and Cs^+ ions, the distance between the metal ions and the DB18C6 cavity is slightly larger than in the case of the K^+ ion,[4] which allows H_2O molecules to interact with the Rb^+ or Cs^+ ion only on top of the M^+•DB18C6 part, providing a single stable conformer. The existence of multiple isomers for the hydrated K^+•DB18C6 complexes can contribute to the effective formation of the K^+•DB18C6 complex and preferential capture of K^+ ion by DB18C6 in solution because of "conformational" entropic effects. These are different from usual entropic effects, which are related to the Gibbs free energy of a single conformation, but the more the number of complex conformers, the more

preferred the complex formation. In this sense, the results of the Rb^+ and Cs^+ complexes reinforce the uniqueness of K^+ ion in the encapsulation by DB18C6.

5. Conclusion

We have measured UVPD spectra of K^+•DB18C6•$(H_2O)_n$, Rb^+•DB18C6•$(H_2O)_n$, and Cs^+•DB18C6•$(H_2O)_n$ (n = 1–8) complexes and IR-UV double-resonance spectra of the Rb^+•DB18C6•$(H_2O)_{1–5}$ and the Cs^+•DB18C6•$(H_2O)_3$ complexes in a cold, 22-pole ion trap. The structure of dominant forms observed in the experiment has been determined or proposed for all the complexes based on the analysis of the UV and IR spectra. Since conformer-specific, IR-UV dip spectra are not available for all the Rb^+•DB18C6•$(H_2O)_n$ and Cs^+•DB18C6•$(H_2O)_n$ complexes, we cannot exclude completely the possibility of other isomers. However, the IR-UV gain spectra, which provide IR bands of all the isomers in the experiment, are well reproduced by calculated spectra of the most stable isomers for the Rb^+ complexes. This suggests that other higher energy isomers, if they exist, are not so abundant in the experiment. The bare complexes (K^+•DB18C6, Rb^+•DB18C6, and Cs^+•DB18C6) have a similar, boat-type conformation, but the distance between the metal ions and the DB18C6 increases with increasing the ion size from K^+ to Cs^+. This structural difference highly affects the manner in which they are hydrated. In the case of the hydrated K^+•DB18C6 complexes, the water molecules can be bound on both sides of the boat-type K^+•DB18C6 structure. In contrast, the H_2O molecules in the hydrated Rb^+•DB18C6 and Cs^+•DB18C6 complexes are located only on top of them. The UV absorption shifts gradually to the low frequency from n = 0 to 4 for the K^+ and Rb^+ complexes and from n = 0 to 5 for the Cs^+ complex, then shifts back to the high frequency at n = 5 for K^+ and Rb^+ and at n = 6 for Cs^+. This spectral trend is related to

the stability of the hydrated complexes of these ions, $M^+•(H_2O)_n$. Addition of one H_2O molecule to the K^+•DB18C6•$(H_2O)_4$, Rb^+•DB18C6•$(H_2O)_4$, or Cs^+•DB18C6•$(H_2O)_5$ complex makes the interaction between the metal ions and the water clusters attached on the boat-type conformers weaker. As a result, the interaction between DB18C6 and the metal ions becomes stronger, and the UV absorption moves back to the higher frequency at n = 5 for the K^+ and Rb^+ complexes and at n = 6 for the Cs^+ complexes. These hydration profiles are characteristic of micro-hydrated systems, where water molecules are bound to the metal ions cooperatively.[25-26] The M^+•DB18C6 complexes in aqueous solutions are surrounded by a number of H_2O molecules on both sides of the boat conformers. However, as can be seen in Figure 1, H_2O molecules will be preferentially bound on top of the boat conformers for the Rb^+•DB18C6 and Cs^+•DB18C6 complexes even in aqueous solutions because they are displaced from the center of the DB18C6 cavity. Because the K^+•DB18C6 complex can accept H_2O molecules on both sides of the boat conformation, we propose that multiple conformations will contribute entropically to the high stability of the K^+•DB18C6 complex in solution and hence the selectivity of DB18C6 for K^+.

Acknowledgment

This work is partly supported by JSPS KAKENHI Grant Number JP16H04098, and the Swiss National Science foundation through grant 200020_165908 and École Polytechnique Fédérale de Lausanne (EPFL). YI and TE thank the support from JSPS through the program "Strategic Young Researcher Overseas Visits Program for Accelerating Brain Circulation". A part of the calculations is performed using Research Center for Computational Science, Okazaki, Japan.

Supporting Information Available: UVPD spectra of the K^+•DB18C6•$(H_2O)_n$, Rb^+•DB18C6•$(H_2O)_n$, and Cs^+•DB18C6•$(H_2O)_n$ (n = 0–8) complexes. Optimized structures of the hydrated K^+•DB18C6, Rb^+•DB18C6, and Cs^+•DB18C6 complexes calculated at the M05-2X/6-311++G(d,p) level. Expanded views of the UVPD spectra of the n = 1 complexes. Positions of the origin band in the UVPD spectra and results of TD-DFT calculations. Full list of authors of ref. 21. This material is available free of charge *via* the internet at http://pubs.acs.org.

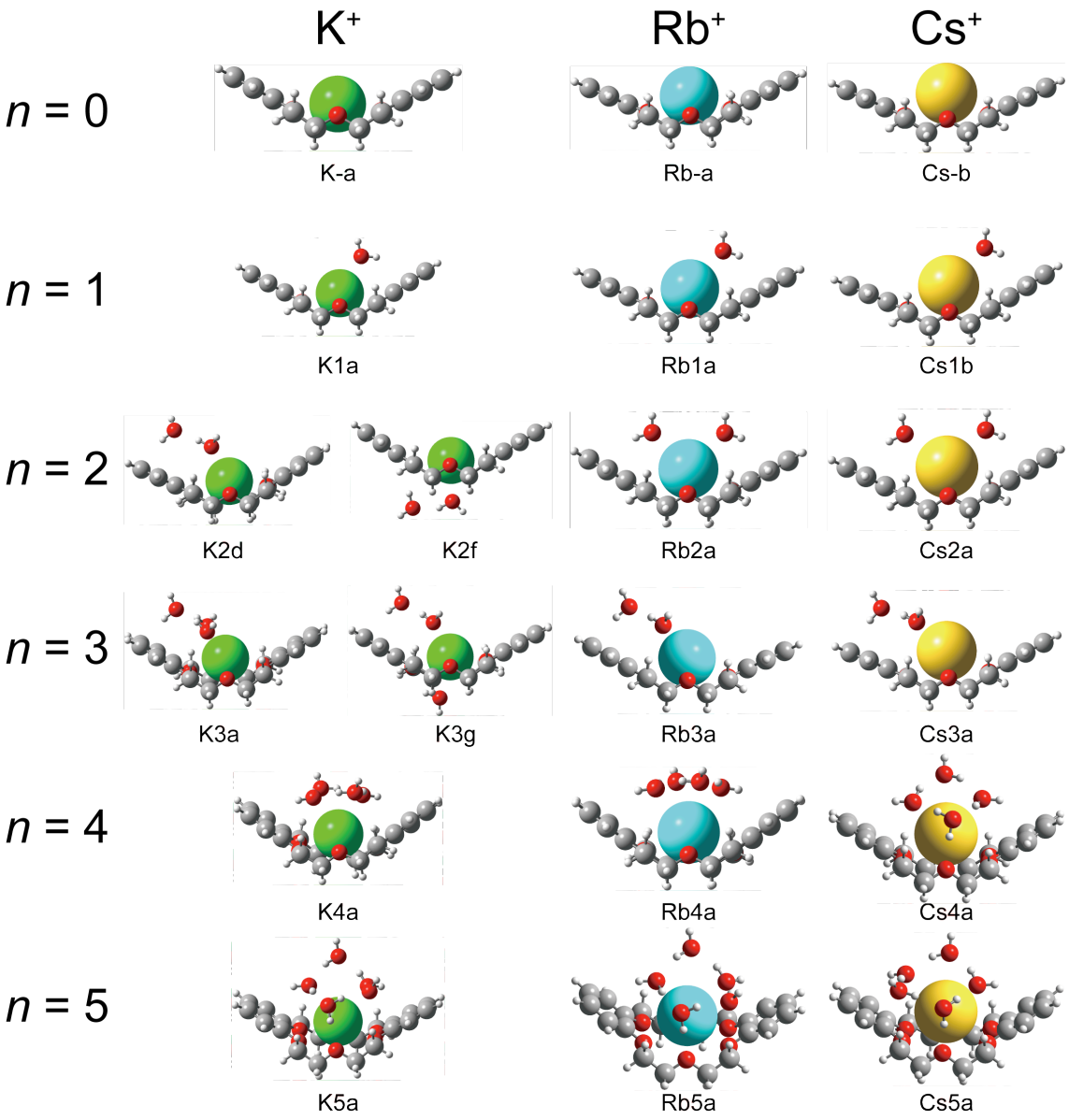

Figure 1. Optimized structures of the M^+•DB18C6•$(H_2O)_n$ (M = K, Rb, Cs; n = 0–5) calculated at the M05-2X/6-311++G(d,p) level. The structures of bare complexes (K-a, Rb-a, and Cs-b) were determined in our gas-phase study (ref. 4). It was confirmed in ref. 6 that the conformers of the K^+•DB18C6•$(H_2O)_{1–5}$ complexes in this figure exist in the experiment under cold gas-phase conditions. For the hydrated Rb^+•DB18C6 and Cs^+•DB18C6 complexes, the most stable conformers (or the second most stable one for Cs^+•DB18C6•$(H_2O)_1$, see text) are displayed in this figure. Other optimized structures of the hydrated complexes are displayed with the relative total energy in the Supporting Information.

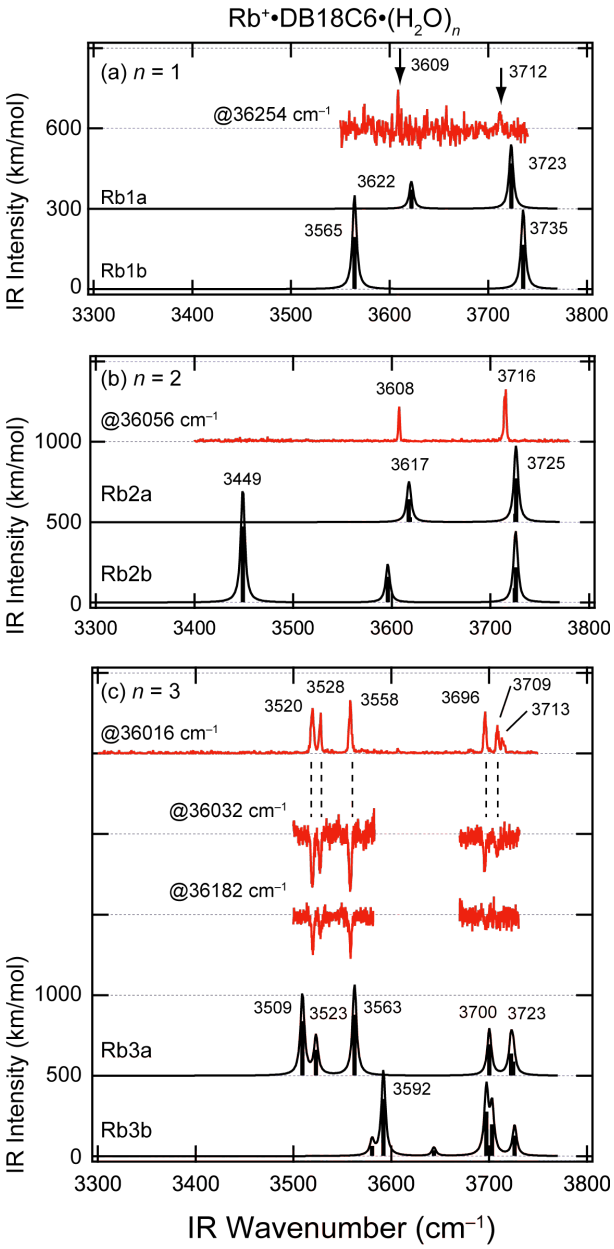

Figure 2. IR-UV (red curves) and theoretical IR (black curves and bars) spectra of the Rb^+•DB18C6•$(H_2O)_{1–3}$ complexes. The UV frequency at which the intensity of fragment ions is monitored for the IR-UV spectra is shown with the arrows in Figure 2S of the Supporting Information.

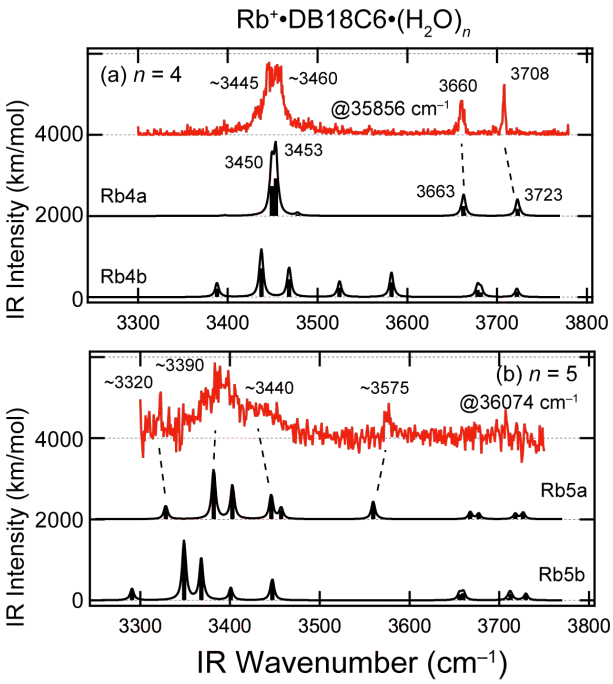

Figure 3. IR-UV (red curves) and theoretical IR (black curves and bars) spectra of the Rb^+•DB18C6•$(H_2O)_{4,\ 5}$ complexes. The UV frequency at which the intensity of fragment ions is monitored for the IR-UV spectra is shown with the arrows in Figure S2 of the Supporting Information.

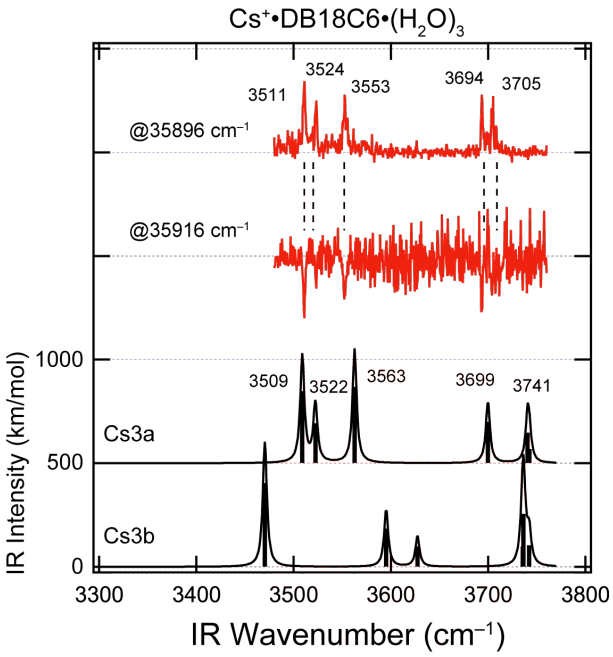

Figure 4. IR-UV (red curves) and theoretical IR (black curves and bars) spectra of the Cs^+•DB18C6•$(H_2O)_3$ complexes. The UV frequency at which the intensity of fragment ions is monitored for the IR-UV spectra is shown with the arrows in Figure S3 of the Supporting Information.

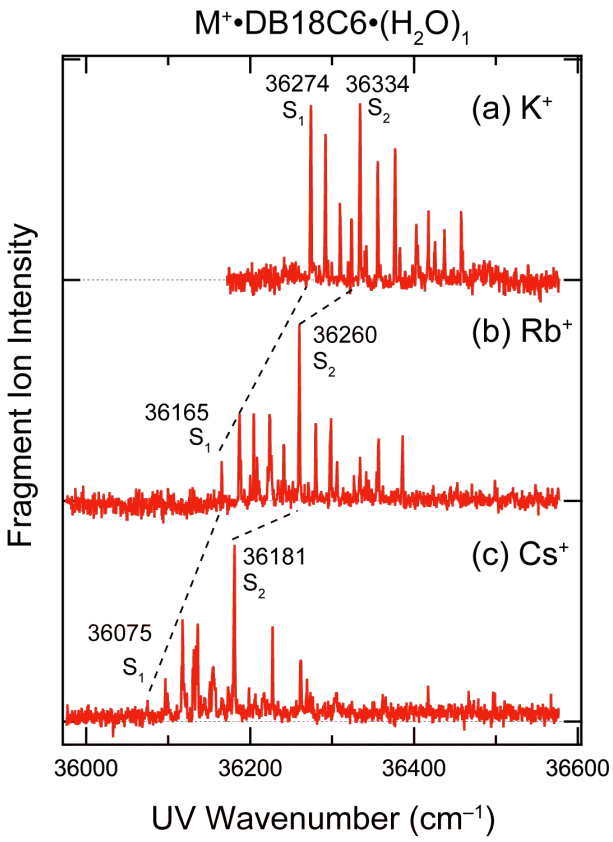

Figure 5. The UVPD spectra of the M^+•DB18C6•$(H_2O)_1$ (M = K, Rb, and Cs) complexes. The intensity of each spectrum is normalized as having the same maximum intensity for all the spectra. The spectrum of the K^+ complex (panel (a)) was taken from ref. 6.

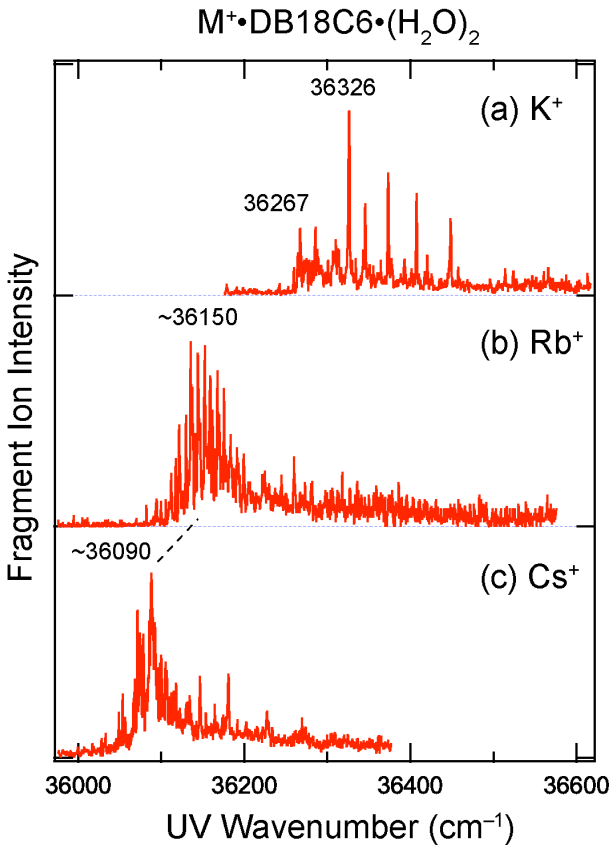

Figure 6. The UVPD spectra of the M^+•DB18C6•$(H_2O)_2$ (M = K, Rb, and Cs) complexes. The intensity of each spectrum is normalized as having the same maximum intensity for all the spectra. The spectrum of the K^+ complex (panel (a)) was taken from ref. 6.

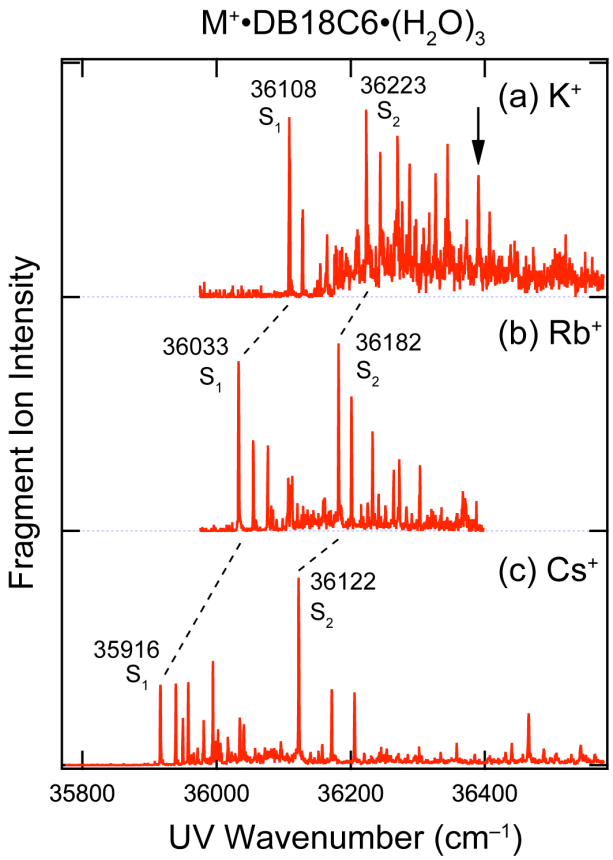

Figure 7. The UVPD spectra of the M^+•DB18C6•$(H_2O)_3$ (M = K, Rb, and Cs) complexes. The intensity of each spectrum is normalized as having the same maximum intensity for all the spectra. The spectrum of the K^+ complex (panel (a)) was taken from ref. 6. A sharp band highlighted with an arrow in panel (a) is assigned to an isomer other than that showing the strong bands at 36108 and 36223 cm^{-1} (ref. 6).

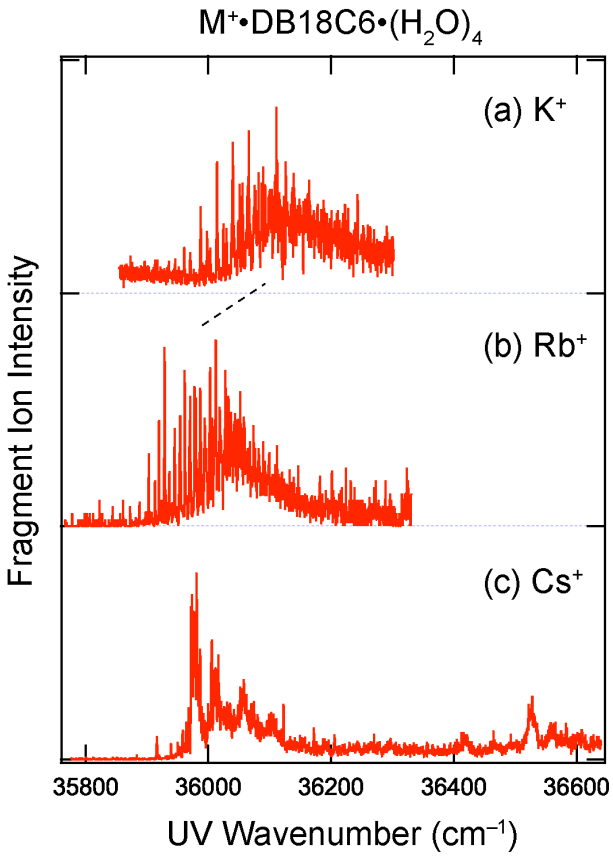

Figure 8. The UVPD spectra of the M^+•DB18C6•$(H_2O)_4$ (M = K, Rb, and Cs) complexes. The intensity of each spectrum is normalized as having the same maximum intensity for all the spectra. The spectrum of the K^+ complex (panel (a)) was taken from ref. 6.

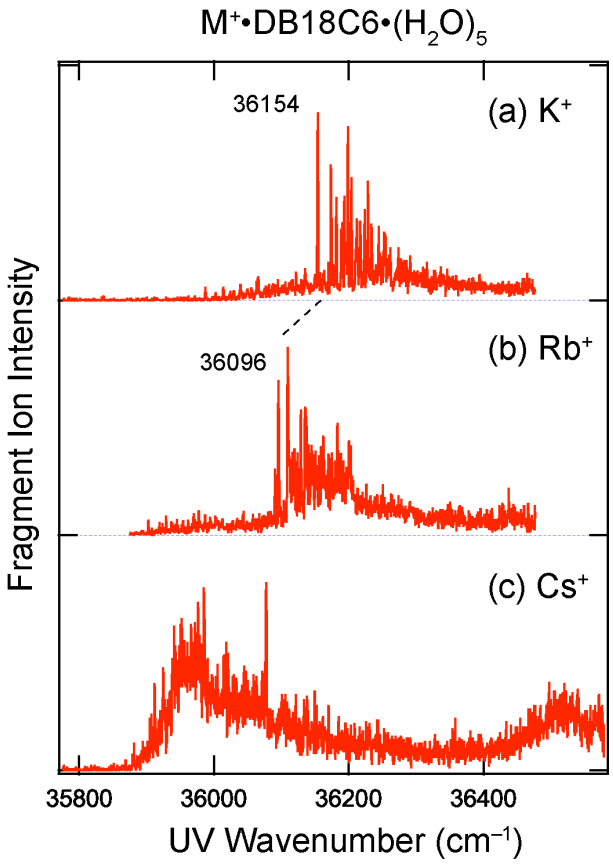

Figure 9. The UVPD spectra of the M^+•DB18C6•$(H_2O)_5$ (M = K, Rb, and Cs) complexes. The intensity of each spectrum is normalized as having the same maximum intensity for all the spectra. The spectrum of the K^+ complex (panel (a)) was taken from ref. 6.

References

(1) Pedersen, C. J. Cyclic Polyethers and Their Complexes with Metal Salts. *J. Am. Chem. Soc.* **1967**, *89*, 7017-7036.

(2) Izatt, R. M.; Bradshaw, J. S.; Nielsen, S. A.; Lamb, J. D.; Christensen, J. J.; Sen, D. Thermodynamic and Kinetic Data for Cation Macrocycle Interaction. *Chem. Rev.* **1985**, *85*, 271-339.

(3) Izatt, R. M.; Terry, R. E.; Haymore, B. L.; Hansen, L. D.; Dalley, N. K.; Avondet, A. G.; Christensen, J. J., Calorimetric Titration Study of Interaction of Several Univalent and Bivalent-Cations with 15-Crown-5, 18-Crown-6, and Two Isomers of Dicyclohexo-18-Crown-6 in Aqueous-Solution at 25 ˚C and μ = 0.1. *J. Am. Chem. Soc.* **1976**, *98*, 7620-7626.

(4) Inokuchi, Y.; Boyarkin, O. V.; Kusaka, R.; Haino, T.; Ebata, T.; Rizzo, T. R., UV and IR Spectroscopic Studies of Cold Alkali Metal Ion-Crown Ether Complexes in the Gas Phase. *J. Am. Chem. Soc.* **2011**, *133*, 12256-12263.

(5) Inokuchi, Y.; Boyarkin, O. V.; Kusaka, R.; Haino, T.; Ebata, T.; Rizzo, T. R., Ion Selectivity of Crown Ethers Investigated by UV and IR Spectroscopy in a Cold Ion Trap. *J. Phys. Chem. A* **2012**, *116*, 4057-4068.

(6) Inokuchi, Y.; Ebata, T.; Rizzo, T. R.; Boyarkin, O. V., Microhydration Effects on the Encapsulation of Potassium Ion by Dibenzo-18-Crown-6. *J. Am. Chem. Soc.* **2014**, *136*, 1815-1824.

(7) More, M. B.; Ray, D.; Armentrout, P. B., Cation-Ether Complexes in the Gas Phase: Bond Dissociation Energies of M^+(Dimethyl Ether)$_x$, x = 1-3, M^+(1,2-Dimethoxyethane)$_x$, x = 1 and 2, and M^+(12-Crown-4) Where M = Rb and Cs. *J. Phys. Chem. A* **1997**, *101*, 7007-7017.

(8) More, M. B.; Ray, D.; Armentrout, P. B. Intrinsic Affinities of Alkali Cations for 15-Crown-5 and 18-Crown-6: Bond Dissociation Energies of Gas-Phase M^+− Crown Ether Complexes. *J. Am. Chem. Soc.* **1998**, *121*, 417-423.

(9) Rodriguez, J. D.; Lisy, J. M. Infrared Spectroscopy of Gas-Phase Hydrated K^+:18-Crown-6 Complexes: Evidence for High Energy Conformer Trapping Using the Argon Tagging Method. *Int. J. Mass Spectrom.* **2009**, *283*, 135-139.

(10) Rodriguez, J. D.; Vaden, T. D.; Lisy, J. M. Infrared Spectroscopy of Ionophore-Model Systems: Hydrated Alkali Metal Ion 18-Crown-6 Ether Complexes. *J. Am. Chem. Soc.* **2009**, *131*, 17277-17285.

(11) Rodriguez, J. D.; Lisy, J. M. Probing Ionophore Selectivity in Argon-Tagged Hydrated Alkali Metal Ion-Crown Ether Systems. *J. Am. Chem. Soc.* **2011**, *133*, 11136-11146.

(12) Inokuchi, Y.; Ebata, T.; Rizzo, T. R. Solvent Effects on the Encapsulation of Divalent Ions by Benzo-18-Crown-6 and Benzo-15-Crown-5. *J. Phys. Chem. A* **2015**, *119*, 8097-8105.

(13) Inokuchi, Y.; Ebata, T.; Rizzo, T. R., UV and IR Spectroscopy of Cold H_2O^+-Benzo-Crown Ether Complexes. *J. Phys. Chem. A* **2015**, *119*, 11113-11118.

(14) Inokuchi, Y.; Nakatsuma, M.; Kida, M.; Ebata, T., Conformation of Alkali Metal Ion-Benzo-12-Crown-4 Complexes Investigated by UV Photodissociation and UV-UV Hole-Burning Spectroscopy. *J. Phys. Chem. A* **2016**, *120*, 6394-6401.

(15) Inokuchi, Y.; Kida, M.; Ebata, T. Geometric and Electronic Structures of Dibenzo-15-Crown-5 Complexes with Alkali Metal Ions Studied by UV Photodissociation and UV-UV Hole-Burning Spectroscopy. *J. Phys. Chem. A* **2017**, *121*, 954-962.

(16) Svendsen, A.; Lorenz, U. J.; Boyarkin, O. V.; Rizzo, T. R. A New Tandem Mass Spectrometer for Photofragment Spectroscopy of Cold, Gas-Phase Molecular Ions. *Rev. Sci. Instrum.* **2010**, *81*, 073107.

(17) Boyarkin, O. V.; Mercier, S. R.; Kamariotis, A.; Rizzo, T. R. Electronic Spectroscopy of Cold, Protonated Tryptophan and Tyrosine. *J. Am. Chem. Soc.* **2006**, *128*, 2816-2817.
(18) Rizzo, T. R.; Stearns, J. A.; Boyarkin, O. V. Spectroscopic Studies of Cold, Gas-Phase Biomolecular Ions. *Int. Rev. Phys. Chem.* **2009**, *28*, 481-515.
(19) Nagornova, N. S.; Rizzo, T. R.; Boyarkin, O. V. Exploring the Mechanism of IR–UV Double-Resonance for Quantitative Spectroscopy of Protonated Polypeptides and Proteins. *Angew. Chem. Int. Ed.* **2013**, *52*, 6002-6005.
(20) Mohamadi, F.; Richards, N. G. J.; Guida, W. C.; Liskamp, R.; Lipton, M.; Caufield, C.; Chang, G.; Hendrickson, T.; Still, W. C. Macromodel - an Integrated Software System for Modeling Organic and Bioorganic Molecules Using Molecular Mechanics. *J. Comput. Chem.* **1990**, *11*, 440-467.
(21) Frisch, M. J.; Trucks, G. W.; Schlegel, H. B.; Scuseria, G. E.; Robb, M. A.; Cheeseman, J. R.; Scalmani, G.; Barone, V.; Mennucci, B.; Petersson, G. A., et al. *Gaussian 09, Revision A.1*, Gaussian, Inc.: Wallingford CT, 2009.
(22) Schuchardt, K. L.; Didier, B. T.; Elsethagen, T.; Sun, L. S.; Gurumoorthi, V.; Chase, J.; Li, J.; Windus, T. L. Basis Set Exchange: A Community Database for Computational Sciences. *J. Chem. Inf. Model.* **2007**, *47*, 1045-1052.
(23) Kusaka, R.; Inokuchi, Y.; Ebata, T. Laser Spectroscopic Study on the Conformations and the Hydrated Structures of Benzo-18-Crown-6-Ether and Dibenzo-18-Crown-6-Ether in Supersonic Jets. *Phys. Chem. Chem. Phys.* **2007**, *9*, 4452-4459.
(24) Kusaka, R.; Kokubu, S.; Inokuchi, Y.; Haino, T.; Ebata, T. Structure of Host-Guest Complexes between Dibenzo-18-Crown-6 and Water, Ammonia, Methanol, and Acetylene: Evidence of Molecular Recognition on the Complexation. *Phys. Chem. Chem. Phys.* **2011**, *13*, 6827-6836.
(25) Miller, D. J.; Lisy, J. M., Hydrated Alkali-Metal Cations: Infrared Spectroscopy and Ab Initio Calculations of $M^+(H_2O)_{X=2-5}Ar$ Cluster Ions for M = Li, Na, K, and Cs. *J. Am. Chem. Soc.* **2008**, *130*, 15381-15392.
(26) Miller, D. J.; Lisy, J. M., Entropic Effects on Hydrated Alkali-Metal Cations: Infrared Spectroscopy and Ab Initio Calculations of $M^+(H_2O)_{X=2-5}$ Cluster Ions for M = Li, Na, K, and Cs. *J. Am. Chem. Soc.* **2008**, *130*, 15393-15404.

TOC Graphic

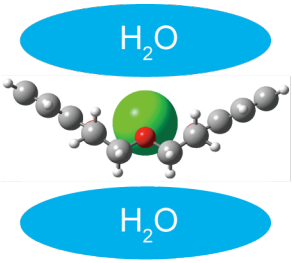

Both sides for K^+

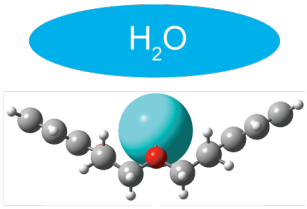

Only top side

for Rb^+ and Cs^+